

# Coherent propagation of small-area pulses in activated crystals

O. P. Varnavskii, V. V. Golovlev, A. N. Kirkin, R. F. Malikov, A. M. Mozharovskii, M. G. Benedikt, and E. D. Trifonov

*P. N. Lebedev Physics Institute, Academy of Sciences of the USSR, Moscow*

(Submitted 1 November 1985)

Zh. Eksp. Teor. Fiz. **90**, 1596–1609 (May 1986)

Theoretical and experimental investigations have been made of coherent propagation of small-area picosecond pulses in neodymium-activated yttrium aluminum garnet (YAG:Nd) and in ruby at 100 K. Changes in the pulse profile during propagation through a population-inverted medium, deviation of the gain from the steady-state Beer value, and transition from coherent to noncoherent amplification as the pulse duration increases were observed. A relationship was established between coherent amplification of small-area pulses and formation of a superradiance pulse in an inverted medium. Amplification of short pulses yielded signals with a profile corresponding to the induced superradiance regime. A change in the pulse profile was also observed when a small-area signal propagated through an absorbing medium. The pulses became shorter in an absorbing ruby sample and the absorption coefficient dropped (compared with the steady-state Beer value) in this case. These propagation regimes could be used in the generation of ultrashort light pulses.

## §1. INTRODUCTION

The profile of a light pulse traveling in a resonant two-level medium changes due to the resonance polarization created by such a pulse in the medium. In the coherent interaction case when the pulse duration  $\tau_p$  is less than the phase relaxation time  $T$  of the medium, the polarization is governed by the electric field not at the relevant moment but in a time interval of order  $T$ . This gives rise to singularities of short light pulses traveling across a medium characterized by slow phase relaxation and to such transient optical effects as the self-induced transparency, photon echo, coherent amplification, etc.<sup>1</sup>

The evolution of a light pulse propagating coherently in an amplifying or absorbing medium is largely governed by its area

$$\theta(x, t) = \frac{\mu}{\hbar} \int_{-\infty}^t E(x, t') dt',$$

where  $\mu$  is the matrix element of the dipole moment of a transition and  $E(x, t)$  is the amplitude of the electric field. In studies of coherent amplification the attention has been concentrated so far on pulses with areas close to the steady-state value  $\theta(x, t) = \pi$ . In particular, in our earlier paper<sup>2</sup> we reported theoretical and experimental studies of coherent amplification of such pulses in activated crystals of ruby and neodymium-activated yttrium aluminum garnet (YAG:Nd) at 100 K. We detected such features of the coherent process as positive and negative oscillations of the field envelope at the trailing edge of an amplified pulse, a doublet structure in the output radiation spectrum, and compression of the time structure of a pulse during amplification.

The case of small-area pulses,  $\theta \ll 1$ , has until recently been almost totally neglected. It has obviously been assumed that it is of no practical interest because amplification increases the area under the pulse profile so that the condition

$\theta \ll 1$  is no longer obeyed. However, it has now become clear that even in this regime, which can be called linear, there are interesting properties which distinguish it from incoherent amplification. As shown in Ref. 3, in this case the growth of a signal obeys a law other than the exponential Beer's law typical of incoherent amplification in the linear regime. This deviation from Beer's law in the case of small-area pulses has been called the laser lethargy or lethargic amplification.<sup>4</sup> It is also noteworthy that coherent amplification of small-area pulses is related directly to the superradiance effect.<sup>5</sup> This relationship can be established by investigating not only the transmission of a weak short pulse, but also the secondary effects due to the resonance polarization which such a pulse leaves behind in the medium.<sup>6</sup>

We shall consider some characteristics of coherent propagation of small-area pulses in inverted media. Preliminary results were published earlier.<sup>6-8</sup>

## §2. THEORY

In a theoretical description of coherent amplification we shall use the Maxwell-Bloch equations for slowly varying amplitudes of the electric field  $E$  and of the polarization  $P$ , which in the one-dimensional case have the following form if the bulk losses and longitudinal relaxation are ignored:

$$\frac{\partial A}{\partial x} = \frac{\Omega}{v} \int_{-\infty}^{\infty} R(t, x, \nu) G(\nu) d\nu, \quad (1a)$$

$$\partial R / \partial \tau = (i\nu - T_2^{-1}) R(t, x, \nu) + 2\Omega A(t, x) Z(t, x, \nu), \quad (1b)$$

$$\partial Z / \partial \tau = -\Omega [A(t, x) R^*(t, x, \nu) + A^*(t, x) R(t, x, \nu)], \quad (1c)$$

where  $\Omega = (2\pi N_0 \hbar \omega_0)^{1/2} \mu / n \hbar$ ;  $\nu = \omega_0 - \omega$ ;  $\omega_0$  is the resonance frequency;  $A = -i\mu E / \hbar \Omega$  is the dimensionless field amplitude;  $R = P / \mu N_0$  is the dimensionless resonance polarization;  $2N_0 Z$  is the population inversion density;  $N_0$  is the initial inversion density;  $\tau = t - x/v$  is the delayed time;  $v$  is the velocity of light in the medium;  $n$  is the refractive

index;  $G(\nu)$  is the inhomogeneous broadening profile;  $T_2$  is the relaxation time of the polarization characterizing homogeneous broadening.

If we consider only small-area pulses which do not affect greatly the inversion of a given transition, the system of equations becomes linear. This is achieved by substituting  $Z = 1/2$  into Eqs. (1a) and (1b).

The linear approximation is usually valid during the very first stage of the process. In particular, it has been used in studies of the statistics of the delay time of superradiance pulses.<sup>9</sup> However, if the phase relaxation is sufficiently rapid that a superradiance pulse does not develop, the linearized system (1) can be used to describe the whole process. It has an analytic solution if the inhomogeneous broadening profile is Lorentzian:

$$G(\nu) = \frac{T_2^*}{\pi(1 + (T_2^*\nu)^2)}, \quad (2)$$

$$A(x, t) = \int_0^\tau \left[ \frac{dA_0(\tau')}{d\tau'} + \frac{1}{T} A_0(\tau') \right] I_0 \left( 2\Omega \left( \frac{x\tau'}{v} \right)^{1/2} \right) \times \exp \left( -\frac{\tau'}{T} \right) d\tau',$$

where  $I_0$  is a modified Bessel function of the zeroth order,  $A_0$  is the amplitude of the input signal ( $x = 0$ ), and

$$T = (1/T_2 + 1/T_2^*)^{-1} \quad (b)$$

is the time representing the total line width allowing both for the homogeneous ( $T_2$ ) and inhomogeneous ( $T_2^*$ ) broadening effects. We can see that in the case of small-area pulses the influence of the Lorentzian inhomogeneous broadening process is indistinguishable from the homogeneous broadening effect. The differences become considerable only when the real line profile is allowed for.

We shall consider an input pulse in the form of a step which appears at the moment  $t = 0$ :  $A_0(t) = E_0\theta(t)$ . For very long relaxation times ( $T \rightarrow \infty$ ) the solution is

$$A(x, t) = A_0 I_0 \left( 2\Omega \left[ \frac{x(t-x/v)}{v} \right]^{1/2} \right) \theta(t-x/v). \quad (3)$$

The quantity  $\tau = t - x/v$  represents the observation time measured from the moment at which the leading edge passes through a cross section at  $x$ . If  $\tau = 0$ , we obtain  $I_0(0) = 1$ , i.e., the leading edge passes through the system without amplification. Since the asymptotic behavior of  $I_0(z)$  for large values of the argument is in the form of  $\exp z$ , then for a fixed  $\tau$  the rise of the amplitude in the limit of large values of  $x$  occurs in accordance with the law

$$A(x, t) = A_0 \exp(2\Omega(\tau x/v)^{1/2}), \quad (4)$$

which corresponds to lethargic amplification. Allowing for the finite phase relaxation time, we find that a step pulse is changed into the following form by amplification:

$$A(x, t) = A_0 I_0 \left( 2\Omega \left( \frac{x\tau}{v} \right)^{1/2} \right) \exp \left( -\frac{\tau}{T} \right) \theta(\tau) + \frac{A_0}{T} \int_0^\tau I_0 \left( 2\Omega \left( \frac{x\tau'}{v} \right)^{1/2} \right) \exp \left( -\frac{\tau'}{T} \right) d\tau'. \quad (5)$$

If  $\tau$  is much greater than  $T$ , then Eq. (5) transforms into

$$A(x, t \rightarrow \infty) = A_0 \exp(Tx\Omega^2/v). \quad (6)$$

This expression represents the usual Beer's law for incoherent amplification and the power gain of this process is  $2T\Omega^2/v$ .

The linearized system of equations obtained by substituting  $Z = 1/2$  in Eq. (1) makes it possible to investigate lethargic amplification in the intermediate case when the interaction should be regarded as coherent, but the area under a pulse remains small because of sufficiently rapid phase relaxation. However, if the phase relaxation is a slow process, it follows that in a study of the radiation emitted as a result of the resonance polarization induced in a medium by a short small-area seed pulse it is necessary to use the complete system (1) which allows for the change in the population inversion. The effect we are discussing here represents the so-called induced superradiance studied theoretically in Ref. 6.

### §3. CALCULATION OF INDUCED SUPERRADIANCE IN YAG:Nd AND IN RUBY

Dicke superradiance (sometimes called superfluorescence<sup>10</sup>) can be regarded as spontaneous radiation because it is initiated by quantum fluctuations of the atomic polarization. It is shown in Ref. 11 that the initial atomic polarization is a Gaussian random process. The corresponding distribution of the initial angles of the Bloch vectors has the average value  $\bar{\theta}_0 \sim 2/N^{1/2}$ , where  $N$  is the total number of inverted atoms in a system emitting light cooperatively. The random nature of the growth of superradiance makes the pulse parameters unstable. For example, the scatter of the delay times of the first intensity maximum can reach 12% of the average value.<sup>9</sup> The delay time can be estimated from<sup>12</sup>

$$\tau_d = (\tau_R/4) |\ln(\bar{\theta}_0/2\pi)|^2, \quad (7)$$

where  $\bar{\theta}_0$  is the average value of the initial angle of rotation of the Bloch vector and  $\tau_R$  is the characteristic superradiance time.<sup>1</sup> A study of the statistics of the delay times made in Ref. 12 showed that Eq. (7) gives the correct order of magnitude of  $\tau_d$ .

We shall consider the case when  $\bar{\theta}_0$  is governed not by the fluctuation statistics, but by external agencies. This can be ensured by transmitting a short pulse of small area (but greater than  $\bar{\theta}_0$ ) through an inverted sample. Such a pulse creates a macroscopic polarization in the medium which initiates a superradiance pulse. Then the initial angle of the Bloch vector at each point in the medium is equal to the area of an initiating pulse passing through this point, so that the delay time can be reduced considerably. An experiment of this kind was carried out in Cs vapor.<sup>13</sup> When the input pulse was sufficiently short ( $\tau_p < \tau_n$ ), it changed little on transmission by this vapor: the field at the maximum increased proportionally to  $\theta_0 x$ . Therefore, the angle  $\theta_0$  was approximately the same for all the atoms in a sample. Under these conditions a superradiance pulse can be described by a self-similar solution of the Maxwell-Bloch equations.<sup>14</sup>

We have investigated the propagation of small-area

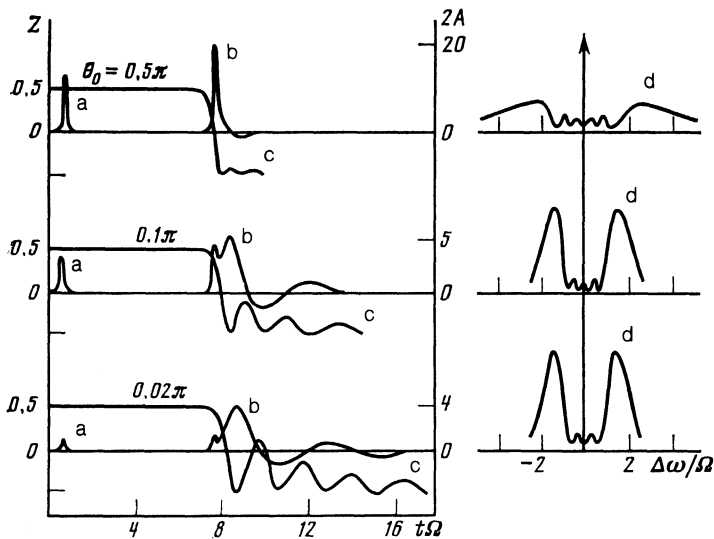


Fig. 1. Influence of the input area  $\theta_0$  on an induced superradiance pulse generated in ruby sample of length 12 cm with an initial inversion density  $4 \times 10^{17} \text{ cm}^{-3}$  in the absence of phase relaxation: a) input pulse  $\tau_p = 0.2\Omega^{-1}$ ; b) output pulse; c) population inversion at the exit end of the sample; d) output pulse spectrum.

pulses theoretically by solving the system (1) numerically. This solution reflects the general laws governing coherent amplification in two-level media. We used dimensionless units in these calculations, but specific results were obtained for the values of the parameters typical of activated crystals of ruby and YAG:Nd (transition wavelengths 0.694 and 1.061  $\mu\text{m}$ ) at a temperature close to 100 K. It was assumed, as usual, that the medium was of the two-level type. This was fully justified in the case of YAG:Nd. Since ruby has a more complex system of levels, several calculations were carried out for a medium with a split lower level. The time scale  $\Omega^{-1}$  used in the calculations was 100 ps for the ruby samples used in the experimental part of the present investigation and 70 ps for YAG:Nd samples. The characteristic superradiance time  $\tau_n$  was 10 and 7 ps, respectively. The input pulse was taken in the Gaussian form. It was assumed that there was not phase modulation.

Figure 1 shows graphs representing the influence of the input area  $\theta_0$  on an induced superradiance pulse generated in a ruby sample. At low values of  $\theta_0$  an initiating pulse of short duration, comparable with  $\tau_R$ , passes through a sample practically without any change. The next self-similar pulse has a characteristic doublet structure, like a pulse of the usual superradiance in an extended sample. When  $\theta_0$  is increased, the superradiance pulse delay decreases and its time structure is compressed. A further rise of  $\theta_0$  causes a superradiance pulse to be superposed on the pulse which initiates it, and a transition takes place to coherent amplification of pulses with an entry area  $\sim \pi$ , investigated in Ref. 2. Note that the oscillatory structure of the field in the relevant graph in Fig. 1 is weak compared with that in the case  $\tau_R < \tau_p \leq T$  discussed in Ref. 2, and that the bulk of the energy is contained in the first maximum of the field.

We now consider the influence of phase relaxation. This factor has an important influence from the experimental point of view, because it is the rate of phase relaxation that determines the possibility of observing induced superradiance in a particular medium. A radiation pulse of area approaching  $\pi$  is formed only if the phase relaxation time

exceeds the superradiance delay time. Superradiance is suppressed as  $T$  is reduced. The effect of inhomogeneous broadening differs from that of homogeneous broadening. This can be judged on the basis of the calculated dependence shown in Fig. 2. If  $T$  is dominated by the inhomogeneous broadening effect, the trailing edge of the first maximum becomes steeper and there is a tendency for field oscillations

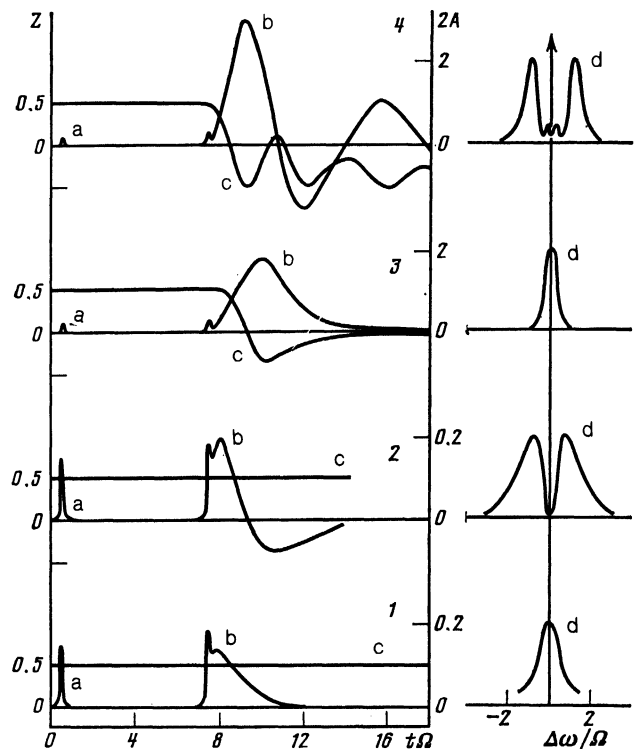


FIG. 2. Influence of phase relaxation on induced superradiance generated in a ruby sample of length 12 cm with an initial inversion density  $4 \times 10^{17} \text{ cm}^{-3}$ : a) input pulse  $\tau_p = 0.1\Omega^{-1}$ ,  $\theta_0 = \pi/200$ ; b) output pulse; c) population inversion at the exit end of the sample; d) spectrum of the output signal; 1)  $T_2 = 0.4\Omega^{-1}$ ,  $T_2^* = \infty$ ; 2)  $T_2 = \infty$ ,  $T_2^* = 0.3\Omega^{-1}$ ; 3)  $T_2 = 2\Omega^{-1}$ ,  $T_2^* = 4\Omega^{-1}$ ; 4)  $T_2 = \infty$ ,  $T_2^* = 4\Omega^{-1}$ .

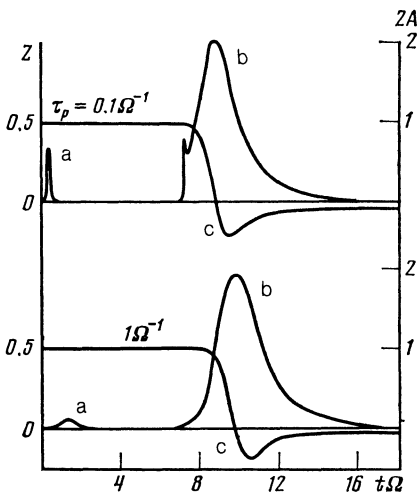


FIG. 3. Transition from induced superradiance to lethargic amplification in ruby with increasing input pulse duration. Length of the sample 12 cm, initial inversion density  $4 \times 10^{17} \text{ cm}^{-3}$ ,  $\theta_0 = \pi/50$ ,  $\alpha L = 5.5$ ,  $T_2 = \Omega^{-1}$ ;  $T_2^* = \infty$ . a) Input pulse; b) output pulse; c) population inversion at the exit end of the sample.

to appear. If the homogeneous broadening effect predominates, the trailing edge is smooth and there are no oscillations.

Therefore, the results of this calculation demonstrate that it should be possible to observe induced superradiance in activated crystals for typical line widths. Under our experimental conditions the process of phase relaxation was governed mainly by the inhomogeneous broadening effect, and the time  $T$  was 15–20 ps for YAG:Nd and 40–50 ps for ruby. It should be noted that superradiance could not be observed under these conditions, because a calculation of the delay times carried out on the basis of Eq. (7) gave 500 ps for YAG:Nd and over 1 ns for ruby. On the other hand, having a phase relaxation time short compared with  $\tau_d$  facilitated accumulation of atoms at the upper level as a result of the relatively slow pumping by flashlamps. (In the absence of phase relaxation the cooperative light emission effects limit considerably the population of the upper level if the excitation time of the medium exceeds  $\tau_d$ —see Ref. 15.) Estimates obtained in Ref. 6 indicate that under our experimental conditions the intensity of the radiation created by the cooperative effects should be less than the intensity of the usual spontaneous radiation emitted in the total solid angle. Therefore, the inversion density at which the pumping effect is balanced by deexcitation is governed only by the emission of amplified spontaneous radiation, which is a relatively slow process.

The calculated results plotted in Fig. 3 illustrate the transition from induced superradiance to lethargic amplification as the duration of the input pulse increases. An increase in the pulse duration causes the radiation due to the polarization which is created in the medium by the input pulse, to be superposed on this pulse. As already pointed out, an input pulse changes little during its passage through an amplifier if it is shorter than  $\tau_R$ . A more rigorous criterion of the existence of a local maximum of the field envelope at the leading edge of the output pulse can be deduced by solving

Eq. (2). In the case of a Gaussian input pulse of the type  $A_0 \exp(-t^2/2\sigma^2)$ , this criterion is

$$\sigma \leq \tau_R. \quad (8)$$

Clearly, such a local maximum may correspond to an input pulse, modified somewhat by the superposition of stimulated superradiance on this pulse. In the limiting case of a very short pulse, its maximum increases by an amount proportional to  $\theta_0 L$ , where  $L$  is the amplification length.

Lethargic amplification is observed for pulses of duration satisfying the condition  $\tau_R < \tau_p < T$ . We can see from Fig. 3 that its characteristic features are lengthening of the pulse during amplification and a small gain compared with that expected on the basis of Beer's law. Both these features can be explained qualitatively by describing the process in terms of the spectral language. The condition  $\tau_p < T$  means that the spectrum of an input pulse is wider than the transition line. The frequency components which do not fall within the line profile are amplified less effectively. Consequently, the power gain is considerably less than that predicted by the exponential Beer's law for the noncoherent case and since the radiation spectrum is then reduced in width, the spectrally limited pulses should become longer. It is interesting that this spectral approach was used earlier to study the formation of a stimulated emission spectrum in the free-running<sup>16</sup> and passive mode-locking<sup>17,18</sup> regimes. Transformation of the field profile in the course of linear amplification, which appears as spectral selection in the spectral description, is identical with lethargic amplification when the description is made in the time domain.

The intensity of amplified pulses was calculated under conditions close to those in our experiments. The results of the calculations are presented in Figs. 4 and 5. In the case of input pulse durations typical of our experimental conditions the calculations indicate the possibility of observation of two fragments in an output signal. However, because of the fast phase relaxation, an induced radiation pulse is strongly suppressed and its area is considerably less than  $\pi$ . If the area of the input pulse is increased, then both fragments of the output pulse merge and a transition takes place to coherent amplification. Induced superradiance pulses with an area close to  $\pi$  can be generated for given input pulse durations if the inhomogeneous line width of a ruby crystal is less than  $0.1 \text{ cm}^{-1}$  and that of a YAG:Nd crystal is less than  $0.3 \text{ cm}^{-1}$ .

The curve in Fig. 6 is obtained allowing for the real structure of the ruby levels when the lower level is split by  $0.38 \text{ cm}^{-1}$ . For phase relaxation times much longer than the reciprocal of the splitting the calculation predicts positive

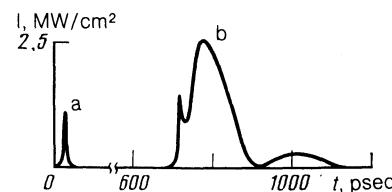


FIG. 4. Calculation of the intensity of a pulse amplified in ruby. Length of the sample 12 cm,  $\alpha L = 5.5$ ,  $T_2 = 200 \text{ ps}$ ,  $T_2^* = 50 \text{ ps}$ ,  $\tau_p = 10 \text{ ps}$ ,  $\theta_0 = \pi/300$ . a) Input pulse; b) output pulse.

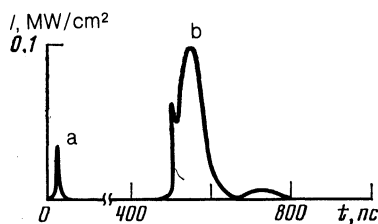


FIG. 5. Calculation of the intensity of a pulse amplified in YAG:Nd. Length of the sample 8 cm,  $\alpha L = 3$ ,  $T_2 = 200$  ps,  $T_2^* = 30$  ps,  $\tau_p = 7$  ps,  $\theta_0 = \pi/200$ . a) Input pulse; b) output pulse.

and negative oscillations of the field envelope at a frequency of  $0.38 \text{ cm}^{-1}$ , which corresponds to 100% modulation of the intensity at the doubled frequency. For values of  $T$  typical of our conditions the modulation is weaker, and we may conclude that the splitting of the lower level does not influence the results significantly. It is interesting to note that in calculating the gain experienced by large-area pulses an allowance for the splitting of the lower level has an even smaller effect than in the case of small-area pulses.

## 4. EXPERIMENTS

### 1. Investigated media and experimental method

We investigated experimentally the amplification of picosecond pulses in YAG:Nd and ruby crystals. To the best of our knowledge, the only experiments on coherent amplification of small-area pulses have been carried out in gases using far infrared radiation.<sup>19</sup> In these experiments it was found that the gain obeys the  $\exp x^{1/2}$  law, but no changes in the pulse profile were reported.

We used samples with almost the same parameters as in the preceding investigation.<sup>2</sup> Rods of YAG:Nd were 8 mm in diameter and 80 mm long, and the concentration of Nd was 0.6%. The small-signal gain  $\alpha L$  obtained for pumping with two IFP-800 flashlamps in a tightly filled illumination enclosure amounted to  $\alpha L \approx 3$ . Ruby rods were 12 mm in diameter and 120 mm long, and the concentration of Cr was  $1.5 \times 10^{19} \text{ cm}^{-3}$ . Two IFP-2000 flashlamps in a tightly packed enclosure were used to pump the ruby and the gain was  $\alpha L \approx 5.5$ . These rods were cooled in a nitrogen vapor stream obtained from a Dewar with liquid nitrogen or in a stream of liquid nitrogen. The temperature of the rods could be varied within the range 80–100 K. The longitudinal temperature distribution varied by less than 2 K. The construction of the laser head was described in detail in Ref. 20.

Estimates of  $T_2$  and  $T_2^*$  were made using the temperature dependences of the widths of the lines representing transitions in the active elements. The data reported in Refs. 21 and 22 for ruby and in Ref. 23 for YAG:Nd, together with the weak temperature dependence of the inhomogeneous width, indicated that when the temperature was increased from 80 to 100 K, the value of  $T_2$  varied within the range 100–300 ps. Under our conditions the line width was governed primarily by the inhomogeneous broadening and it amounted to  $\sim 1 \text{ cm}^{-1}$  in the case of YAG:Nd and  $\sim 0.3 \text{ cm}^{-1}$  in the case of ruby, which corresponded to  $T_2^* = 20$

and 60 ps, respectively.

A laser with an Nd-activated silicate glass active element operating in the passive mode locking regime was the source of input pulses in the experiments on the amplification in YAG:Nd. The laser emission wavelength was tuned by an intracavity Fabry-Perot interferometer with a base 0.1 mm long, which made it possible to vary the emission line wavelength within a band  $\sim 50 \text{ cm}^{-1}$  wide. Rough frequency tuning was performed by an STÉ-1 spectrograph. Fine tuning was carried using the maximum amplification in the YAG:Nd rod. The tuning error was less than  $\sim 0.1 \text{ cm}^{-1}$ . The source of input pulses in the case of a ruby amplifier was a ruby laser operated at a low temperature in the passive mode-locking regime.<sup>24</sup> The time parameters of the radiation were determined employing an image converter camera with a time resolution of  $\sim 20$  ps. The camera slit was covered by a multistage attenuator, which extended the dynamic range of the camera.

### 2. Lethargic amplification and induced superradiance

We investigated the dependence of the output signal on the area of the input signal for various pulse durations. The value of  $\theta_0$  was estimated from the pulse duration and the energy, and it was varied by neutral optical filters as well as with a dense ( $\leq 1\%$ ) saturable filter (in the case of ruby, a solution of cryptocyanin in ethanol; in the case of YAG:Nd, a solution of dye 3274u in dichloroethane), which also ensured an effective reduction in the pulse duration.<sup>25</sup> Densitograms of the pulses representing amplification in ruby at 80 K were recorded (Fig. 7). The input pulse profile was distorted in these densitograms because the resolution of the image converter camera was insufficient. Nevertheless, the results in this figure indicated that the duration of the input pulses decreased from the top to the bottom. In the topmost densitogram the input pulse was considerably wider than the instrumental function of the camera and its duration exceeded  $\tau_R$ . According to the calculations reported above, this corresponded to lethargic amplification. The experiments confirmed the characteristics of the amplification predicted by the numerical calculation, i.e., an increase in the pulse duration and a gain which was low compared with that predicted by Beer's law. The peak radiation power increased only by a factor of  $\sim 10$ . In the two lower densitograms the duration of the input pulses approached  $\tau_R$ . The output pulses exhibited fragments corresponding to the input pulses

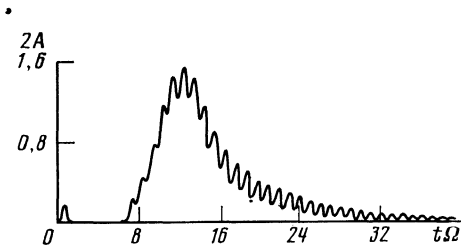


FIG. 6. Calculation of the amplitude of the field amplified in ruby, allowing for the splitting of the lower level by  $0.38 \text{ cm}^{-1}$ . Length of the sample 12 cm, initial inversion density  $4 \times 10^{17} \text{ cm}^{-3}$ ,  $T_2 = \Omega^{-1}$ ,  $T_2^* = \infty$ ,  $\tau_p = 0.5\Omega^{-1}$ .

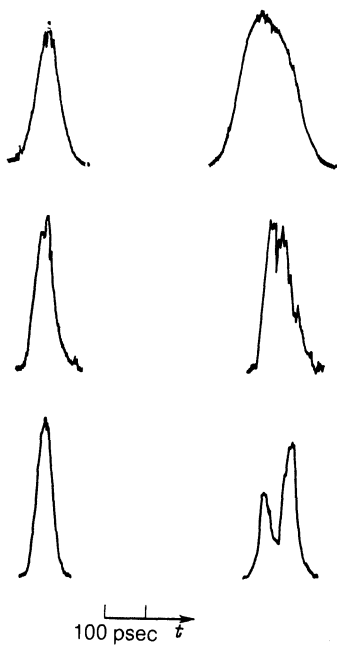


FIG. 7. Experimental densitograms of the amplification in ruby at 80 K;  $L = 12$  cm,  $\alpha L \approx 5.5$ . The input pulses are shown on the left and the output pulses on the right.

and to superradiance pulses suppressed strongly because of fast phase relaxation. Allowing for the instrumental broadening of the first fragment of the output signal, it was found that the agreement between the experimental data and the results of numerical calculations shown in Fig. 4 was satisfactory.

The densitogram obtained on amplification in YAG:Nd is shown in Fig. 8. The change in the signal profile was in agreement with the calculations (Fig. 5) if an allowance was made for the finite resolution of the image converter camera and it could also be explained by manifestation of the induced superradiance effect, weakened by fast phase relaxation. The energy gain in the experiments on YAG:Nd was less than 10 even in the case of tuning to the center of the gain profile, and this value was considerably less than the steady-state gain.

The image converter camera study was accompanied by measurements by the two-photon luminescence method. It was established that the minimum duration of the input pulses was 8 ps. A study of cross-correlation of the input and output signals showed that the leading fragment of the output signal traveled at the velocity of light and, consequently, the second fragment was delayed, as expected in the case of induced superradiance.

### 3. Interference effects in amplification of pulses with oscillatory envelopes

The presence of delayed secondary radiation gives rise to interesting interference effects between such radiation and the field of an input pulse if the envelope of the pulse field exhibits positive and negative oscillations. We showed earlier<sup>2</sup> that such an oscillatory structure develops in the course of coherent amplification of large-area pulses. The

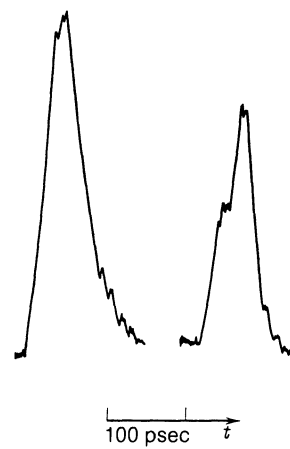


FIG. 8. Experimental densitograms of the amplification in YAG:Nd at 100 K;  $L = 8$  cm,  $\alpha L \approx 3$ . The input pulse is shown on the left and the output pulse on the right.

interference effects may be very useful in the formation of high-power ultrashort pulses in amplifiers. As pointed out in Refs. 26 and 27, if the amplifier is long, the output pulse should be close to the self-similar solution and almost independent of the initial conditions. About half the energy of such a pulse (the actual amount depends on the initial conditions) may be contained in a second pulse which follows the maximum peak and does not contribute to the peak radiation power. The time scale of a self-similar pulse is related to the field amplitude and changes in a correlated manner during amplification. When such a correlation is disturbed by, for example, a change in the field amplitude, the interference effects described above are observed.

Figure 9a shows densitograms of the amplification in ruby of an input pulse of  $\sim \pi/20$  area and with an oscillatory structure. The duration of the pulse considerably exceeded  $\tau_R$  and, therefore, a radiation pulse due to the induced polar-

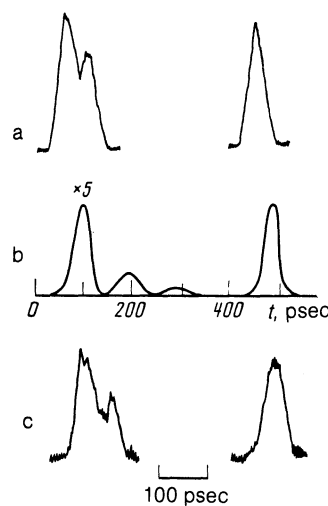


FIG. 9. a) Amplification in ruby at 100 K;  $L = 12$  cm,  $\alpha L \approx 5.5$ ,  $\theta_0 \approx \pi/20$  (experimental results). b) Amplification in ruby;  $L = 12$  cm,  $T_2 = 150$  ps,  $T_2^* = 20$  ps,  $\alpha L = 6$ ,  $\theta_0 = \pi/3$  (calculations). c) Amplification in ruby at 100 K;  $L = 12$  cm,  $\alpha L \approx 5.5$ ,  $\theta_0 \approx \pi/3$  (experimental results).

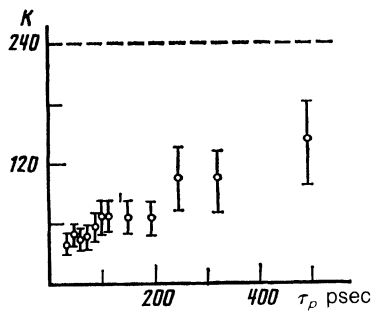


FIG. 10. Dependence of the energy gain on the duration of the input pulses.

ization was superimposed on the input pulse and interfered with the latter. The interference within the first oscillation of the envelope was constructive, whereas in the second oscillation it was destructive. Therefore, the second peak in the output pulse was suppressed.

In some cases suppression of the second pulse was observed also in the case of large-area pulses. The suppression mechanism involved interference, but in the present case a simpler interpretation is possible. It is known that the first portion of the self-similar pulse is of area which tends to  $2\pi$ . The total area of the remaining oscillations is close to  $-\pi$ . If the pulse area is reduced by a factor  $\sim 2$ , the area of the first fragment is close to  $\pi$  and it consumes all the inversion, so that the subsequent oscillations are weakened. When the amplifier is sufficiently long, the final result is the formation of a self-similar pulse. However, selection of the amplifier length can ensure maximum suppression of the second pulse. Figures 9b and 9c show the results of a calculation of the amplification of a self-similar pulse with a weakened field amplitude and the experimental densitograms obtained under conditions assumed in the calculations. These results indicate that second pulse can be effectively suppressed by a suitable selection of the amplifier length and of the input pulse area.

#### 4. Transition from coherent to noncoherent amplification

It is clear from Eq. (5) that when a rectangular pulse is propagating, its leading edge changes in accordance with the lethargic amplification law. However, at times of the order of  $T$  a steady-state Beer gain is established, i.e., a transition takes place from coherent to incoherent amplification. It should be mentioned straight away that we are considering small areas under the pulses:  $\theta(x, T) \ll 1$ . Otherwise a pulse can affect significantly the population inversion and formation of a square-wave pulse can begin.

Establishment of steady-state amplification was investigated theoretically in Ref. 8. We studied experimentally the transition from coherent to incoherent amplification in ruby. Input pulses with a steep leading edge were used and changes in their profile as a result of amplification were recorded, together with the deviation of the gain from the steady-state value in the case of pulses of different durations. Pulses of the required shape were supplied to the amplifier input by passing ruby laser radiation through a saturable filter in order to shorten the leading edge of the signal and

suppress oscillations of its trailing edge, followed by attenuation in neutral filters and passage through a Fabry-Perot interferometer which lengthened the trailing edge of the pulse. Variation of the base length of the interferometer and of the reflection coefficients of its mirrors made it possible to vary the pulse duration at the amplifier input within the range  $\sim 40$ – $500$  ps. The area of the input pulses was  $\approx \pi/200$  and that of the amplified pulses was less than  $\approx \pi/20$ , i.e., the change in the population could be ignored. The pulse energy was measured with calorimeters.

In the case of pulses of duration considerably greater than  $\tau_R$  the leading edge became longer. In the time domain the deformation of the leading edge can be explained by the finite time needed for the development of a coherent macroscopic polarization in the investigated medium. In the frequency domain this deformation corresponds to distortion of a wide-band signal due to its passage through a narrow-band amplifier. The instantaneous power gain is not constant in a pulse and it increases toward the end of the pulse.

Figure 10 shows the experimental dependence of the energy gain on the laser pulse duration. Shorter pulses corresponded to a lower gain. When the input pulse duration was  $< T$ , the gain depended weakly on the duration because growth of the induced superradiance and lengthening of the pulses took place under these conditions. When the pulse duration became greater than  $T$ , coherent amplification became noncoherent and the gain approached the steady-state value of 240. This dependence was in qualitative agreement with the theoretical representations developed in Refs. 3 and 8. However, in the case of the longest pulses the measured values could be underestimated because of the imperfect spectral selection by the Fabry-Perot interferometer and because of residual modulation of the input radiation. These circumstances prevented us from comparing the measured values of the gain quantitatively with those found by calculations, although there was a very definite overall tendency for the gain to rise with increasing pulse duration.

It is interesting to note that a similar time dependence of the gain was manifested when pulses with a leading edge

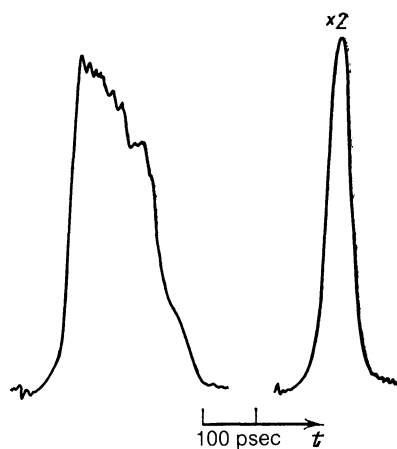


FIG. 11. Transmission of a  $\theta_0 \approx \pi/100$  pulse by an absorbing ruby sample with  $\exp \alpha L \approx 200$ . The input pulse is shown on the left and the output pulse on the right.

steeper than  $T$  propagated across an absorbing medium. Figure 11 shows a densitogram obtained during the passage of a pulse of  $\approx \pi/100$  area with a steep leading edge through an absorbing ruby sample at 100 K, characterized by the maximum Beer absorption of  $\sim 200$  at the line center. We used the same ruby crystal as in the amplifier experiment. However, the plane of polarization of the radiation was parallel to the optical axis, because in the case of perpendicular polarization the optical thickness of the sample was far too great. By analogy with the inverted medium, the amplification increased with the time between the pulses because in this case the absorption appeared some time after the transition from lethargic amplification to noncoherent absorption. The peak power of the output pulse fell by just a factor of  $\sim 2$ , but the change in the energy was considerable because of the strong reduction in the duration. This pulse shortening could be used in generation of ultrashort pulses. It is clear from the densitogram that shortening by a factor of five took place in this case. As in the inverted sample, we could propose a simple spectral explanation of the observed changes in the profile: the spectral components corresponding to the central part of the absorption band were absorbed first and the emission spectrum was broadened, which corresponded to pulse shortening.

Coherent propagation of small-area pulses in an absorber had been investigated earlier<sup>28,29</sup> and deviations from Beer's law were recorded. In these investigations the pulse durations were considerably less than  $T$  and there was no process of establishment of steady-state absorption.

## §5. DISCUSSION OF RESULTS

We investigated in detail coherent amplification of small-area pulses by theoretical analysis and various experimental methods. The results obtained made it possible to determine the relationship between coherent amplification of small-area pulses and formation of superradiance in pulses in an inverted medium. It was shown theoretically that a self-similar pulse of induced superradiance can be obtained on excitation of homogeneous polarization of a medium by a pulse of duration less than or of the order of the superradiance time. This regime could not be observed in its pure form in our experiments because of the strong inhomogeneous broadening in the investigated samples. Nevertheless, the use of a seed pulse created favorable conditions in principle for the generation of a self-similar pulse in media in which spontaneous superradiance can be generated.

In practice these regimes may be useful in the generation of high-power ultrashort pulses. It would be interesting to construct systems combining coherent and noncoherent propagation regimes. The small signal area does not imply a low radiation intensity, because the area under a pulse is governed by the field amplitude and by the dipole moment of

the transition. The same signal may have a large area in one medium and a small area in another medium (or, as in the case of ruby, a large area for one polarization and a small area for another polarization). This makes it possible to combine, in the formation of pulses, the large- and small-area pulse regimes using characteristic features of both regimes.

The authors are grateful to M. D. Galanin and A. M. Leontovich for their interest and encouragement, and to A. A. Kosterev for his help in the experiments.

- <sup>1</sup>L. Allen and J. H. Eberly, *Optical Resonance and Two-Level Atoms*, Wiley, New York, 1975 (Russ. transl., Mir, Moscow, 1978).
- <sup>2</sup>O. P. Varnavskii, A. N. Kirkin, A. M. Leontovich, R. F. Malikov, A. M. Mozharovskii, and E. D. Trifonov, *Zh. Eksp. Teor. Fiz.* **86**, 1227 (1984) [*Sov. Phys. JETP* **59**, 716 (1984)].
- <sup>3</sup>M. D. Crisp, *Phys. Rev. A* **1**, 1604 (1970).
- <sup>4</sup>F. A. Hopf, P. Meystre, M. O. Scully, and J. F. Seely, *Phys. Rev. Lett.* **35**, 511 (1975).
- <sup>5</sup>R. H. Dicke, *Phys. Rev.* **93**, 99 (1954).
- <sup>6</sup>R. F. Malikov and E. D. Trifonov, *Opt. Commun.* **52**, 74 (1984).
- <sup>7</sup>O. P. Varnavskii, V. V. Golovlev, A. N. Kirkin, and A. M. Mozharovskii, *Pis'ma Zh. Eksp. Teor. Fiz.* **41**, 9 (1985) [*JETP Lett.* **41**, 8 (1985)].
- <sup>8</sup>M. G. Benedikt and E. D. Trifonov, *Opt. Spektrosk.* **59**, 161 (1985) [*Opt. Spectrosc. (USSR)* **59**, 95 (1985)].
- <sup>9</sup>F. Haake, J. W. Haus, H. King, G. Schröder, and R. Glauber, *Phys. Rev. A* **23**, 1322 (1981).
- <sup>10</sup>R. Bonifacio and L. A. Lugiato, *Phys. Rev. A* **11**, 1507 (1975).
- <sup>11</sup>R. Glauber and F. Haake, *Phys. Lett. A* **68**, 29 (1978).
- <sup>12</sup>N. Skribanowitz, I. P. Herman, J. C. MacGillivray, and M. S. Feld, *Phys. Rev. Lett.* **30**, 309 (1973).
- <sup>13</sup>Q. H. F. Vrehen and M. F. H. Schuurmans, *Phys. Rev. Lett.* **42**, 224 (1979).
- <sup>14</sup>D. C. Burnham and R. Y. Chiao, *Phys. Rev.* **188**, 667 (1969).
- <sup>15</sup>J. C. MacGillivray and M. S. Feld, *Phys. Rev. A* **23**, 1334 (1981).
- <sup>16</sup>A. M. Leontovich and V. L. Churkin, *Zh. Eksp. Teor. Fiz.* **59**, 7 (1970) [*Sov. Phys. JETP* **32**, 4 (1971)].
- <sup>17</sup>B. Ya. Zel'dovich and T. I. Kuznetsova, *Usp. Fiz. Nauk* **106**, 47 (1972) [*Sov. Phys. Usp.* **15**, 25 (1972)].
- <sup>18</sup>P. G. Kryukov and V. S. Letokhov, *IEEE J. Quantum Electron.* **QE-8**, 766 (1972).
- <sup>19</sup>A. T. Rosenberger, H. K. Chung, and T. A. DeTemple, *IEEE J. Quantum Electron.* **QE-20**, 523 (1984).
- <sup>20</sup>A. M. Leontovich and A. M. Mozharovskii, *Tr. Fiz. Inst. Akad. Nauk SSSR* **98**, 3 (1977).
- <sup>21</sup>D. E. McCumber and M. D. Sturge, *J. Appl. Phys.* **34**, 1682 (1963).
- <sup>22</sup>D. F. Nelson and M. D. Sturge, *Phys. Rev.* **137**, A1117 (1965).
- <sup>23</sup>T. Kushida, *Phys. Rev.* **185**, 500 (1969).
- <sup>24</sup>O. P. Varnavskii (Varnavsky), A. N. Kirkin, A. M. Leontovich, R. G. Mirzoyan, A. M. Mozharovskii (Mozharovsky), and I. I. Solomatina, *Opt. Commun.* **45**, 342 (1983).
- <sup>25</sup>W. Krause, *Opt. Commun.* **48**, 47 (1983).
- <sup>26</sup>V. E. Zakharov, *Pis'ma Zh. Eksp. Teor. Fiz.* **32**, 603 (1980) [*JETP Lett.* **32**, 589 (1980)].
- <sup>27</sup>S. V. Manakov, *Zh. Eksp. Teor. Fiz.* **83**, 68 (1982) [*Sov. Phys. JETP* **56**, 37 (1982)].
- <sup>28</sup>S. M. Hamadani, J. Goldhar, N. A. Kurnit, and A. Javan, *Appl. Phys. Lett.* **25**, 160 (1974).
- <sup>29</sup>H.-J. Hartmann and A. Laubereau, *Opt. Commun.* **47**, 117 (1983).

Translated by A. Tybulewicz